Inorganic Chemistry

Article

pubs.acs.org/IC

Modulating the Sensor Response to Halide Using NBD-Based Azamacrocycles

Stefano Amatori,[‡] Gianluca Ambrosi,[†] Elisa Borgogelli,[†] Mirco Fanelli,[‡] Mauro Formica,[†] Vieri Fusi,*[,†] Luca Giorgi,[†] Eleonora Macedi,[§] Mauro Micheloni,[†] Paola Paoli,[§] Patrizia Rossi,[§] and Aurora Tassoni[‡]

[†]Department of Base Sciences and Fundamentals, Chemistry Section, University of Urbino "Carlo Bo", P.zza Rinascimento 6, I-61029 Urbino, Italy

[‡]Department of Biomolecular Sciences, Molecular Pathology Laboratory "PaoLa", University of Urbino "Carlo Bo", Via Arco d'Augusto 2, I-61032 Fano, Italy

[§]Department of Industrial Engineering, University of Florence, Via S. Marta 3, I-50139 Firenze, Italy

Supporting Information

ABSTRACT: Ligand **L** (2,6-bis{[7-(7-nitrobenzo[1,2,5]oxadiazole-4-yl)-3,10-dimethyl-1,4,7,10-tetraazacyclododeca-1-yl]methyl}phenol) is a fluorescent sensor that is useful for detecting Cu(II), Zn(II), and Cd(II). Some of the complexes formed are able to sense the presence of halides in solution. **L** passes through the cellular membrane, becoming fluorescent inside cells. The $H_{-1}L^{-}$ species is able to form dinuclear complexes with $[M_2H_{-1}L]^{3+}$ stoichiometry with Cu(II), Zn(II), and Cd(II) ions, experiencing a CHEF effect upon metal coordination in an acetonitrile/water 95:5 (v/v) solution. In all three of the complexes investigated, the metal cations are coordinatively unsaturated and can therefore bind secondary ligands as anionic species. The crystal structure of $[Cd_2(H_{-1}L)Cl_2](ClO_4)\cdot 4H_2O$ is discussed. The Zn(II) complex behaves as an OFF−ON sensor for fluoride and chloride anions.

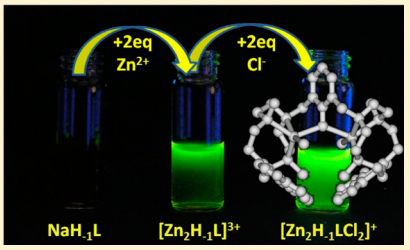

INTRODUCTION

There is a growing need to improve optical chemosensors that are able to detect halides, particularly chloride, in various types of biological and environmental samples.[1−9] The detection of these chemical species is an important target for monitoring both their excessive levels and their deficiencies in natural resources. Over the last century, the production and application of halide-containing compounds took on an ever greater importance in many fields, such as medicine, dentistry, plastics, pesticides, food, and photography. As a consequence, new halogen-containing compounds have come into everyday use. Halide sensors can be synthesized by linking a photoactive fragment to the receptor, achieving highly selective and sensitive chemosensors. However, these systems generally respond to the presence of halides by fluorescence quenching.[10] Indeed, there are still very few known examples of chemosensors that are able to sense chloride by enhancing their fluorescence. There have recently been reports on interesting examples of OFF−ON fluorescent sensors for Cl^- based on rotaxane displacement,[11] a chemosensing ensemble approach,[12] and a metallo-receptor.[13]

In a previous paper, we described the synthesis and properties of ligand **L1** (Chart 1) that contains the NDB fluorophore 7-nitrobenzo[1,2,5]oxadiazole-4-yl, which is linked to a cyclen-derived polyamino macrocycle.[13,14] This ligand has interesting photochemical properties and is suitable for use in metal sensing and for the assemblage of metallo-receptors that are able to sense halide anions. The $[ML1]^{2+}$ species, with M(II)=Cu(II), Zn(II), or Cd(II), behaves as a sensor for halide anions by changing its fluorescent emission. In particular, the $[CuL1]^{2+}$ and $[ZnL1]^{2+}$ species were quenched upon the addition of halide, which corresponds well with the working feature of PET-regulated metallo-receptors, whereas the $[CdL1]^{2+}$ complex undergoes strong fluorescence enhancement. Identifying this nonclassic behavior was the main result of our previous study, and we also demonstrated that the key to this interesting property is the involvement in metal coordination of the nitrogen atom that is linked to the NBD moiety. In fact, the strength of the interaction of this nitrogen

Chart 1. Schematic Drawings of L and L1[a]

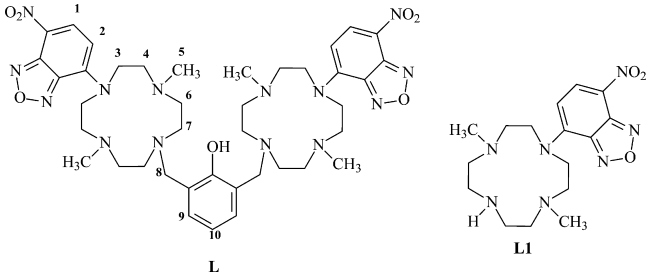

L L1

[a]Numbers refer to the labeling of the C and H atoms in the NMR spectra.

Received: January 30, 2014
Published: April 23, 2014

   dx.doi.org/10.1021/ic5001649 | Inorg. Chem. 2014, 53, 4560−4569

Scheme 1

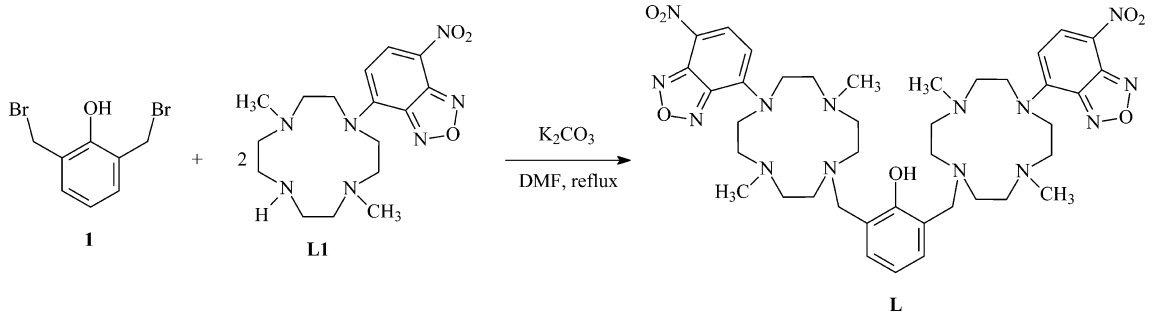

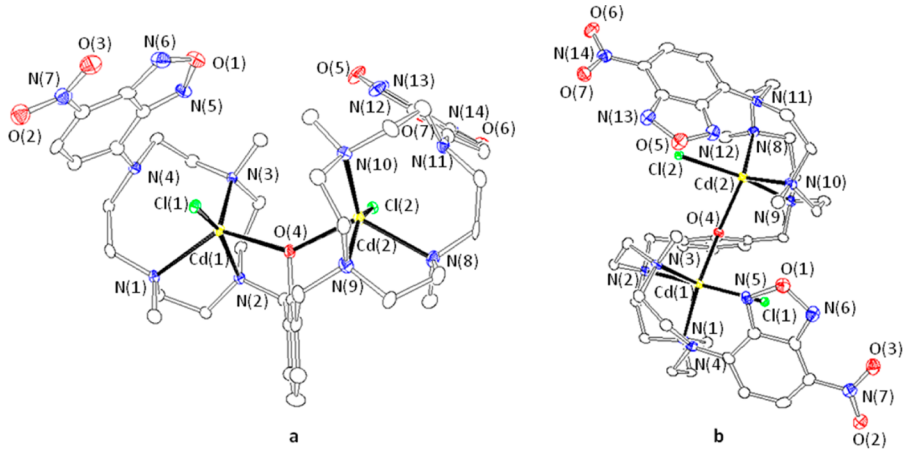

Figure 1. ORTEP3 front (a) and top (b) views together with the atom labeling of the $[Cd_2(H_{-1}L)Cl_2]^+$ cation of **2**. Ellipsoids are drawn at 30% probability. Hydrogen atoms have been omitted for clarity.

atom with the metal ion regulates both the population of the emitting CT excited state as well as the arrangement of the NBD system with respect to the macrocyclic plane upon excitation. Our studies confirm that by weakening the (NBD)N−M interaction in the metal complexes an increase in fluorescence emission would be expected. Consequently, when the interaction of the metal complex with an anionic species mainly affects this bond rather than the other M−N bonds, the ligand undergoes fluorescence enhancement because of the CT excited state (in the case of the $[CdL1]^{2+}$ complex). Meanwhile, when the coordination of an external species results in a weakening of the bond between the metal center and the aliphatic amines, PET-induced quenching occurs (in the case of the $[CuL1]^{2+}$ and $[ZnL1]^{2+}$ complexes). On the basis of these results, we concluded that a ligand similar to **L1**, with a molecular topology that is able to force the metal to be closer to the three aliphatic amines of the macrocycle, could be a good strategy for producing a system that is able to sense halides with an OFF−ON mechanism.

Because we have experience with phenol-containing ligands and macrocyclic sensors, we designed and synthesized ditopic ligand **L** (Chart 1), which contains two **L1** units linked to the 2,6 positions of a phenol with two methylene spacers, exploiting the presence in **L1** of an easily functionalized secondary amine function. It is well-known that the phenol moiety of this kind of ligand can be easily deprotonated to obtain an anionic species that is able to form dinuclear metal complexes with $[M_2(H_{-1}L)]^{3+}$ stoichiometry[15−21] in which the two metal ions are forced to be close together by the oxygen atom of the phenolate, which coordinates them in a bridge disposition. This arrangement favors the cooperation of the two metals in coordinating an external guest that can be further bound in a bridge disposition. Crucial to this point is the great tendency of the phenolate oxygen atom to bind two transition-metal ions in a bridge disposition.

In the $[M_2(H_{-1}L)]^{3+}$ species and because of its tendency to act as a bridge, the phenolate framework should maintain the two metal ions close to the aliphatic zone of the two **L1** fragments. This enables the decoordination of the (NBD)N atom as a response to anion addition, giving rise to an increase in the fluorescence emission. The new ligand is able to bypass the cell membrane and to switch on its fluorescence inside the cells, thus giving **L** appeal as a chemosensor for biological use.

SYNTHESIS OF THE LIGAND

Ligand **L1** was synthesized as previously reported.[14] Ligand **L**, meanwhile, was synthesized in good yield by coupling two units of **L1** with 2,6-bis(bromomethyl)phenol (**1**) in DMF in the presence of K_2CO_3 as a base (Scheme 1). Compound **1** was synthesized from 2,6-bis(bromomethyl)anisole by deprotecting the phenolic group with boron tribromide.[22] The reaction between **L1** and **1** produces ligand **L** without further deprotection steps. The ligand was further purified as its octahydrochloride salt and recrystallized from a water/ethanol mixture. To obtain the anionic form of **L**, an aqueous solution of **L**·8HCl was treated with sodium carbonate up to pH 11 and extracted with dichloromethane. The evaporation of the solvent produced pure $NaH_{-1}L$, which was suitable for photochemical and NMR studies.

dx.doi.org/10.1021/ic5001649 | Inorg. Chem. 2014, 53, 4560−4569

RESULTS AND DISCUSSION

Crystal Structure. In the dinuclear complex cation of $[Cd_2(H_{-1}L)Cl_2](ClO_4)\cdot 4H_2O$ (**2**), both of the cadmium ions are pentacoordinated by three nitrogen atoms from the two cyclen moieties, a chloride anion, and the oxygen atom belonging to the phenolate unit. As expected, the latter bridges the metal ions (Figure 1) and keeps them 4.2110(6) Å apart (the Cd(1)−O(4)−Cd(2) angle is 139.5(2)°).[23] The coordination geometry around each Cd(II) is intermediate between the square pyramid and the trigonal bipyramid (τ = 0.503 for Cd(1) and 0.497 for Cd(2)).[24] Cd(1) and Cd(2) are displaced by 1.3213(4) and 1.3250(4) Å, respectively, from the mean planes defined by the four nitrogen atoms of each cyclen moiety (vs 0.8882(4) and 0.586(2)−0.5734(9) Å in parent complexes $[ZnL1Cl]^+$,[13] $[CuL1Cl]ClO_4$, and $[CuL1Cl]PF_6\cdot H_2O$),[14] as previously predicted on the basis of the data deposited in the Cambridge Structural Database, CSD v. 5.34.[25]

The Cd−Cl, Cd−O, and Cd−N bonds are within the expected range for analogous pentacoordinated cadmium complexes (CSD data). However, the bonds involving the nitrogen atom bearing the phenolate moiety (N(2) and N(9)) are definitely longer with respect to the other Cd−N distances (Table 1). As was already found in related complex $[ZnL1Cl]^+$,[13] the nitrogen atoms bearing the NBD moiety, namely, N(4) and N(11), are definitely far from the metal ions (3.067(6) and 3.096(7) Å for Cd(1) and Cd(2), respectively). In fact, both distances are significantly longer than both a typical Cd−N_{amine} length and than the sum of the covalent and ionic radii of nitrogen and cadmium, respectively.[26a] However, given that they are a little shorter than the sum of their van der Waals radii (3.13 Å),[26b−d] the Cd(1)···N(4) and Cd(2)···N(11) contacts could be described as secondary intramolecular interactions, as has been already reported for the related zinc complex.[13] However, this sort of weak Cd···N interactions has been noted already in other cadmium complexes.[27] Moreover, the weak coordinative nature of N(4) and N(11) is also suggested by the sums of the bond angles around them (350.5(6) and (352.0(7)° for N(4) and N(11), respectively), indicating their partial sp^2 hybridization.[28]

Table 1. Selected Distances and Angles for Compound 2

bond distances (Å)		angles (deg)	
Cd(1)−N(1)	2.342(5)	N(1)−Cd(1)−N(2)	75.2(2)
Cd(1)−N(2)	2.415(5)	N(1)−Cd(1)−N(3)	114.4(2)
Cd(1)−N(3)	2.316(5)	N(2)−Cd(1)−N(3)	78.8(2)
Cd(1)−O(4)	2.239(4)	O(4)−Cd(1)−N(1)	128.0(2)
Cd(1)−Cl(1)	2.489(2)	O(4)−Cd(1)−N(2)	82.6(2)
Cd(1)···N(4)	3.067(6)	O(4)−Cd(1)−N(3)	106.3(2)
Cd(2)−N(8)	2.351(5)	O(4)−Cd(1)−Cl(1)	88.9(1)
Cd(2)−N(9)	2.418(6)	Cl(1)−Cd(1)−N(1)	94.7(1)
Cd(2)−N(10)	2.316(6)	Cl(1)−Cd(1)−N(2)	158.2(1)
Cd(2)−O(4)	2.250(4)	Cl(1)−Cd(1)−N(3)	123.0(1)
Cd(2)−Cl(2)	2.490(2)	N(8)−Cd(2)−N(9)	75.5(2)
Cd(2)···N(11)	3.096(7)	N(8)−Cd(2)−N(10)	114.0(2)
		N(9)−Cd(2)−N(10)	79.4(2)
		O(4)−Cd(2)−N(8)	126.4(2)
		O(4)−Cd(2)−N(9)	82.1(2)
		O(4)−Cd(2)−N(10)	108.6(2)
		O(4)−Cd(2)−Cl(2)	87.6(1)
		Cl(2)−Cd(2)−N(8)	93.9(1)
		Cl(2)−Cd(2)−N(9)	156.2(1)
		Cl(2)−Cd(2)−N(10)	124.3(2)

The geometrical disposition of each NBD moiety with respect to the macrocyclic base can be described by the angles between the planes defined by N(4)/N(11) and the carbon atoms of the cyclen ring that are directly linked to each of them (planes A and C in the following) and the mean planes formed by all of the non-hydrogen atoms of the NBD moieties (B and D for the NBD unit related to Cd(1) and Cd(2), respectively). The A/B and C/D angles are 29.0(5) and 24.7(3)°, respectively (L_{in} conformation, according to the nomenclature reported in ref 13), as predicted by a previous simple modeling study on the parent $[CdL1Cl]^+$ complex.[13] A similar arrangement of the NBD moiety (the five-membered ring points toward the coordinating area) characterizes the solid-state structure of related compound $[ZnL1Cl](ClO_4)$[13] (Supporting Information, Figure S1), where the corresponding A/B angle is 37.1(1)°. In contrast, in the analogous $[CuL1Cl](ClO_4)$ and $[CuL1Cl](PF_6)\cdot H_2O$ species, the A/B angle is 89° and the five-membered ring points outside the macrocyclic cavity ($L1_{out}$ conformation).[14] As has been already found[13] for the simpler $[CdL1Cl]^+$ species, for the dinuclear cadmium complex, the L_{in} arrangement of the NBD moiety about the metal cations is by far the most energetically preferable with respect to that of L_{out}, as was found from a geometry optimization[29] of complex cations $[Cd_2(H_{-1}L_{in})C_{l2}]^+$ and $[Cd_2(H_{-1}L_{out})Cl_2]^+$. Finally, in compound **2**, the L_{in} disposition allows two weak contacts to be formed involving N(5) and N(12) and a hydrogen atom from the closest methyl groups (C···N length mean value, 3.413 Å).

Overall, the relative arrangement of the planes containing the cyclen, the NBD, and the phenolate moieties confers a general S-shape to the complex (Figure 1b) that is stabilized by the formation of weak contacts involving the chloride anion and a benzylic hydrogen atom as well as an H atom provided by the closest aliphatic carbon of the cyclen unit from the other half of the complex (C···Cl length mean value, 3.782 Å).

Finally, in the crystal packing of **2**, dimers are formed; partners are connected through the atoms O(3), N(6), and O(1W) (N(6)···O(1W) = 2.94(1) Å and O(3)···O(1W)′ = 2.97(2) Å, where ′ = $-x + 3, -y, -z + 1$; Supporting Information, Figure S2). These dimers interact with water molecules that are all connected with each other. Weak hydrogen-bond interactions connect the water molecules to the perchlorate anion (Figure S2).

Solution Studies. *Metal Complexes. UV−Vis and Fluorescence Studies.* The absorption spectrum of $NaH_{-1}L$ in acetonitrile/water 95:5 (v/v) shows the two typical bands of 4,7-disubstituted benzofurazan moieties at 347 nm ($\varepsilon = 1.6 \times 10^4$ $cm^{-1}\cdot mol^{-1}\cdot dm^3$), which is associated with the $\pi-\pi^*$ transition, and at 490 nm ($\varepsilon = 4.3 \times 10^4$ $cm^{-1}\cdot mol^{-1}\cdot dm^3$), which is attributed to intramolecular charge transfer transitions (CT)[30] (Figure 2a). In this medium, $NaH_{-1}L$ is very weakly fluorescent (λ_{em} = 543 nm, $\Phi_{em} < 0.01$), and the low fluorescence quantum yield can be explained in terms of PET from the lone pair of the nonconjugated nitrogen atoms of the macrocycles to the CT excited state of NBD.[14]

By adding Zn(II) or Cu(II) perchlorate to a solution of $NaH_{-1}L$ in acetonitrile/water 95:5 (v/v), the two absorption maxima undergo a blue shift, and the displacement ends when 2 equiv of metal ions are added. When taking into account the ditopic structure of the ligand, this means that stable dinuclear metal complexes were formed. The positions of the absorption bands, with a ratio M(II)/L of 2:1, were found at 455 (ε = 2.6

dx.doi.org/10.1021/ic5001649 | Inorg. Chem. 2014, 53, 4560−4569

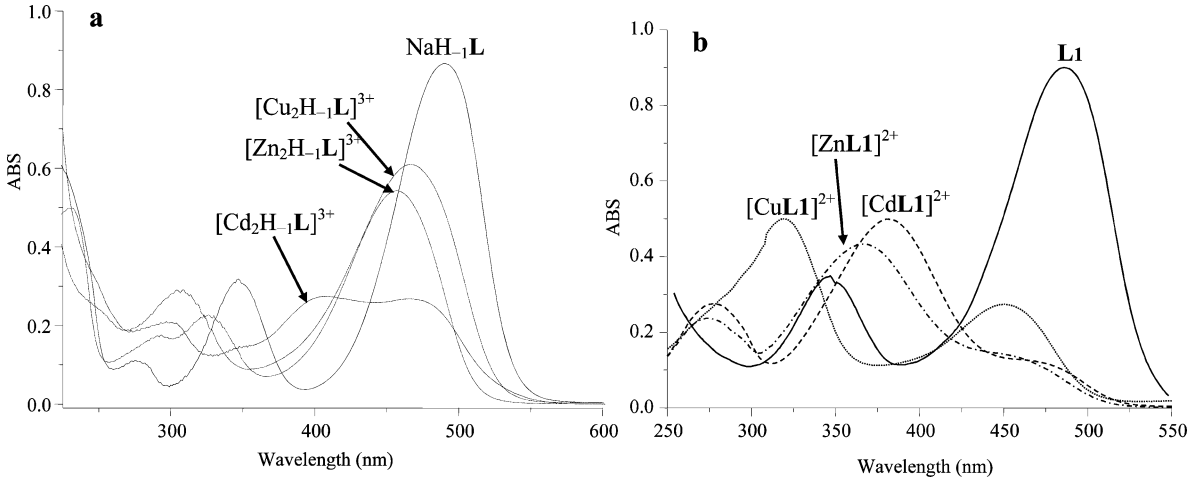

Figure 2. (a) UV−vis spectra of 2.0×10^{-5} mol·dm^{-3} solutions of $NaH_{-1}L$, $[Zn_2H_{-1}L]^{3+}$, $[Cd_2H_{-1}L]^{3+}$, and $[Cu_2H_{-1}L]^{3+}$ in acetonitrile/water 95:5 (v/v). (b) UV−vis spectra of 5.0×10^{-5} mol·dm^{-3} solutions of **L1**, $[ZnL1]^{2+}$, $[CdL1]^{2+}$, and $[CuL1]^{2+}$ in acetonitrile/water 95:5 (v/v).

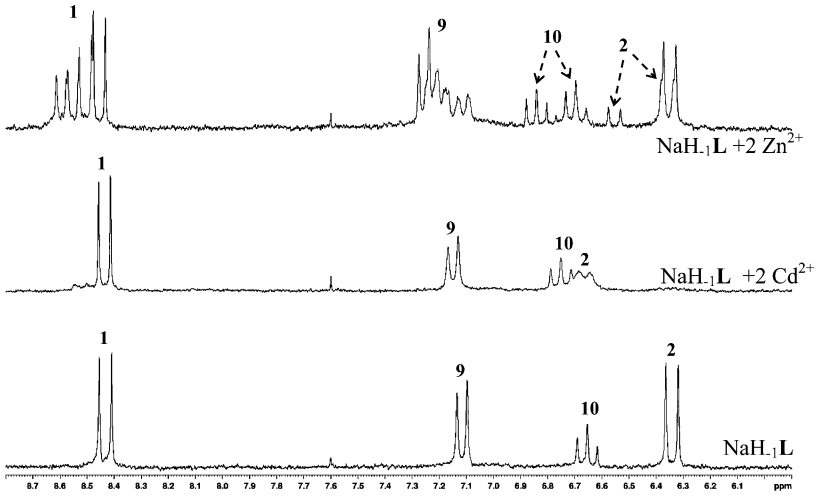

Figure 3. Aromatic part of the ^{1}H NMR spectra of the $NaH_{-1}L$, $[Zn_2H_{-1}L]^{3+}$, and $[Cd_2H_{-1}L]^{3+}$ species in CD_3CN at 298 K. $[NaH_{-1}L] = 1.0 \times 10^{-2}$ mol·dm^{-3} and $[M(II)] = 2.0 \times 10^{-2}$ mol·dm^{-3}.

$\times 10^4$ cm^{-1}·mol^{-1}·dm^3) and 327 nm ($\varepsilon = 1.1 \times 10^4$ cm^{-1}·mol^{-1}·dm^3) for Zn(II) and at 462 ($\varepsilon = 3.3 \times 10^4$ cm^{-1}·mol^{-1}·dm^3) and 331 nm ($\varepsilon = 1.5 \times 10^4$ cm^{-1}·mol^{-1}·dm^3) for Cu(II) (Figure 2a). In these experiments, the shape of the spectra remains unchanged by the addition of the metal ions (Figure 2a), and the only effect is the shift of all of the bands toward higher energy. On the contrary, the absorption spectrum of $NaH_{-1}L$ undergoes a major change when the Cd(II) ion is added; in fact, the band at 347 nm disappears, whereas that at 490 nm shifts to 457 nm ($\varepsilon = 1.5 \times 10^4$ cm^{-1}·mol^{-1}·dm^3) and strongly decreases in absorption and a new band at 403 nm ($\varepsilon = 1.2 \times 10^4$ cm^{-1}·mol^{-1}·dm^3), in the zone of $\pi-\pi^*$ transitions, appears. (Figure 2a). Also, in this case, the spectrum stops changing after the addition of 2 equiv of Cd(II), highlighting the full formation of a stable dinuclear species. The different behavior exhibited by the coordination of Cd(II) suggests a different involvement of the N(NBD) atom in the stabilization of the metal ion. A comparison between the absorption spectra of the mononuclear complexes of **L1** and those of the dinuclear complexes of **L** can be helpful to understand the coordination properties of the latter ligand (Figure 2). The absorption spectra of free **L1** and $NaH_{-1}L$ are very similar. The addition of Cu(II), Zn(II), and Cd(II) to **L1** causes the disappearance of the CT band at 490 nm, and this is because of the involvement of the N(NBD) atom in the coordination of the metal ion.[13] Instead, upon addition of Cu(II) or Zn(II) ions (2 equiv) to a solution of $NaH_{-1}L$, the CT band does not disappear, but it undergoes a blue shift with only a slight decrease of ε. This behavior suggests that in the Cu(II) and Zn(II) complexes of **L** the N(NBD) atom contributes much less to the stabilization of the metal ions than in the parent complexes of **L1**. In the case of the Cd(II) complex of $NaH_{-1}L$, the perturbation of the band at 490 nm for **L** is more significant, and this, together with the appearance of the band at 403 nm, suggests that in this species the N(NBD) atom is involved in the stabilization of the metal ion.

As expected and in agreement with the behavior of **L1**, the addition of Cu(II), Zn(II), or Cd(II) to a solution of $NaH_{-1}L$ strongly increases the intensity of the emission band at 543 nm (Supporting Information, Figure S3). The increase in the fluorescence upon metal coordination can be explained by the inhibition of PET resulting from the involvement of the macrocycle nitrogen atoms in the stabilization of the metal ions. The emission band underwent only a slight blue shift for all of the metal ions tested. This is because the (NBD)N−M interaction in the excited state is less strong than in the

dx.doi.org/10.1021/ic5001649 | Inorg. Chem. 2014, 53, 4560−4569

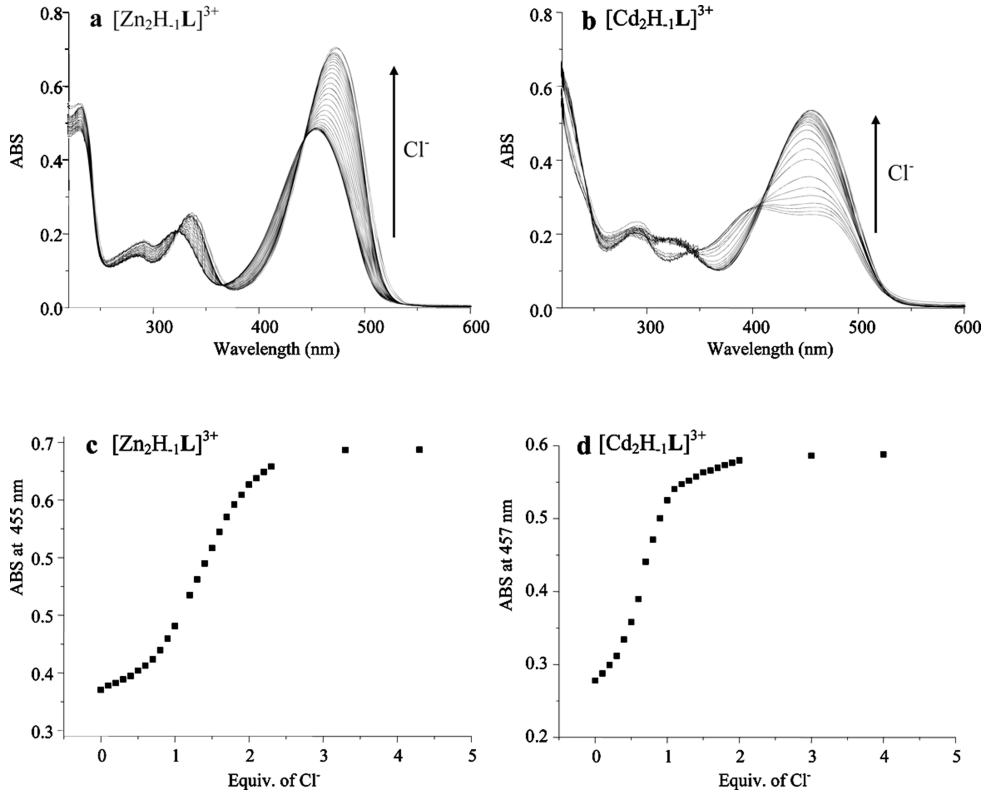

Figure 4. UV−vis titration of $[Zn_2H_{-1}L]^{3+}$ (a) and $[Cd_2H_{-1}L]^{3+}$ (b) with Bu_4NCl in acetonitrile/water 95:5 (v/v) at 298 K. Trend of the absorption at 455 nm for the $[Zn_2H_{-1}L]^{3+}/Cl^-$ system (c) and at 457 nm for the $[Cd_2H_{-1}L]^{3+}/Cl^-$ system (d). $[M_2H_{-1}L^{3+}] = 2.0 \times 10^{-5}$ mol·dm^{-3} and $[Cl^-] = 0 \rightarrow 1.0 \times 10^{-4}$ mol·dm^{-3}.

fundamental state.[13] However, the presence of the positive metal ion destabilizes the emitting CT excited state through an electrostatic interaction.

NMR Spectroscopy Studies. The ^{1}H NMR spectrum of $NaH_{-1}L$ in acetonitrile-d_3 has six aliphatic and four aromatic resonances (Supporting Information, Figure S4): a singlet at δ = 2.23 ppm that integrates 12 protons attributed to the resonance of H5 (H5, 12H); two overlapping broad signals at δ = 2.57 and 2.60 ppm (H6 and H7, 16H); a sharp triplet at δ = 2.92 ppm (H4, 8H); a singlet at δ = 3.58 ppm (H8, 4H); a broad triplet at δ = 4.22 ppm (H3, 8H); a doublet at δ = 6.34 ppm (H2, 2H); a triplet at δ = 6.54 ppm (H10, 1H); a doublet at 7.12 ppm (H9, 2H); and a doublet at δ = 8.43 ppm (H1, 2H). This indicates C_{2v} symmetry for the $H_{-1}L^-$ anion that is mediated on the NMR time scale. The position of the H10 signal confirms that the phenol is present in solution in the deprotonated form.[15] The ^{1}H NMR spectra of $[Zn_2H_{-1}L]^{3+}$ and $[Cd_2H_{-1}L]^{3+}$, which were obtained by adding 2 equiv of M(II) as a perchlorate salt to a solution of $NaH_{-1}L$ in acetonitrile, exhibited a downfield shift of all of the aliphatic and H9 and H10 aromatic resonances. This suggests the involvement of all six aliphatic amine functions and the phenolate moiety in the coordination of M(II).

Upon examining the aromatic part of the ^{1}H NMR spectra of $NaH_{-1}L$, $[Zn_2H_{-1}L]^{3+}$, and $[Cd_2H_{-1}L]^{3+}$ (Figure 3), only one species is present for the $2Cd/H_{-1}L$ system, whereas at least three species in a slow exchange on the NMR time scale are recognized for the $2Zn/H_{-1}L$ system. The resonances of the H9 and H10 protons were strongly perturbed, denoting the involvement of the phenolate oxygen atom in the metal coordination, whereas the displacement downfield of the H1 resonance in some species suggests the possibility of an interaction between the Zn(II) ions and the oxadiazole moiety of the NBD. In contrast, the resonance of H2 was not significantly displaced, suggesting that in the species that prevail in solution the (NBD)N atom is not involved in metal coordination, in agreement with the UV−vis studies.

As already stated, the $2Cd/H_{-1}L$ system contains only one species in solution. In the ^{1}H NMR spectrum, the main perturbation resulting from metal coordination was observed for the sharp resonance doublet of H2, which undergoes a strong downfield shift from δ = 6.34 ppm to δ = 6.67 ppm and changes shape, becoming a broad doublet. This denotes the involvement of the (NBD)N atom in the stabilization of Cd(II), in agreement with the UV−vis data.

All of the UV−vis, fluorescence, and NMR spectra reach their invariance with the addition of 2 equiv of the metal ion investigated. This is due to the high stability of the complexes formed, which, together with the complexity of the $2Zn/H_{-1}L$ system, prevents the determination of the stability constants for the species using such methods.

Anion Recognition. Taking into account the topology of the ligand and the coordination requirement of the metal ions investigated, the $2M(II)/H_{-1}L$ system can be a promising metal-based host for secondary ligands. With this in mind, we explored the behavior of the $2M(II)/H_{-1}L$ systems (M = Cu, Zn, and Cd) as hosts for the halide series.

UV−Vis and Fluorescence Studies. By adding halide anions to all of the dinuclear metal complexes, both the absorption and emission spectra undergo significant changes. The experiments were carried out by adding the selected halide anion as a

dx.doi.org/10.1021/ic5001649 | Inorg. Chem. 2014, 53, 4560−4569

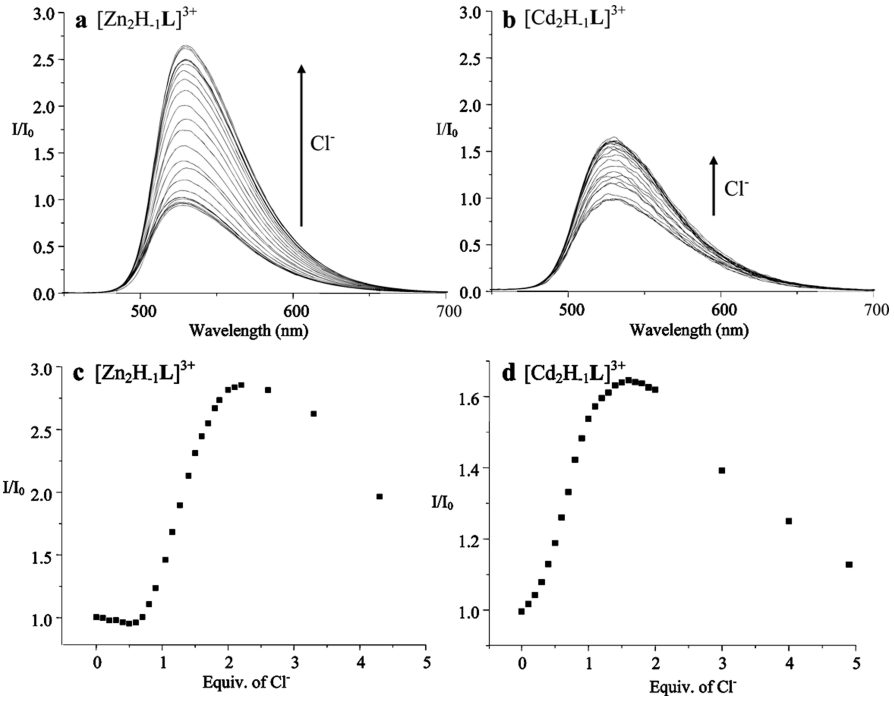

Figure 5. Fluorescence titration of $[Zn_2H_{-1}L]^{3+}$ (a) and $[Cd_2H_{-1}L]^{3+}$ (b) with Bu_4NCl in acetonitrile/water 95:5 (v/v) at 298 K. Trend of the relative emission at 543 nm for the $[Zn_2H_{-1}L]^{3+}/Cl^-$ system (λ_{ex} = 325 nm) (c) and for the $[Cd_2H_{-1}L]^{3+}/Cl^-$ system (λ_{ex} = 310 nm) (d). $[M_2H_{-1}L^{3+}] = 5.0 \times 10^{-6}$ mol·dm^{-3} and $[Cl^-] = 0 \rightarrow 2.5 \times 10^{-5}$ mol·dm^{-3}.

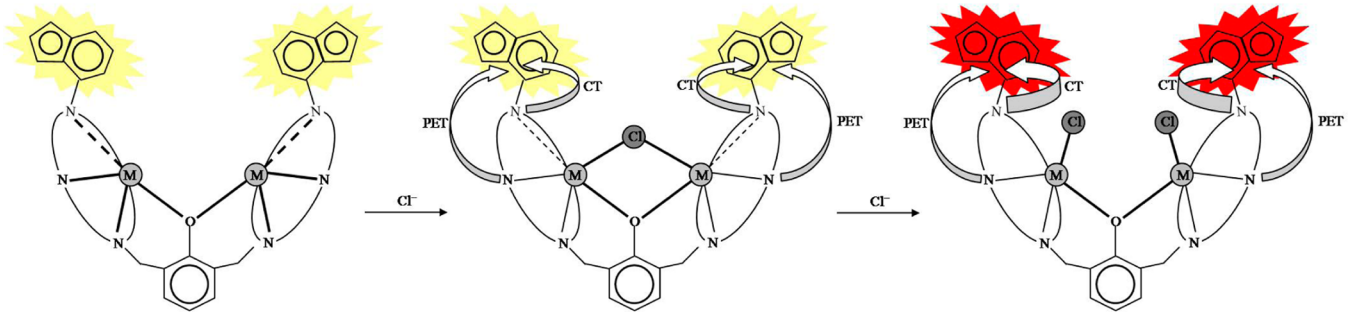

Figure 6. Proposed mechanism for the signal transduction upon halide coordination.

tetrabuthylammonium salt to a solution of preformed $[M_2H_{-1}L]^{3+}$ complexes in acetonitrile/water 95:5 (v/v).

$[Zn_2H_{-1}L]^{3+}$. The addition of halide anions to a solution of $[Zn_2H_{-1}L]^{3+}$ in acetonitrile causes a red shift of the absorption bands that is consistent with the decrease of the interaction between the metal ion and the (NBD)N donor atom upon anion coordination. In fact, the CT band at 453 nm shifts to 472 nm, corresponding to a red shift of 889 cm^{-1} after the addition of an excess (5 equiv) of fluoride, chloride, or bromide anions (Figure 4 and Supporting Information, Figure S5). The addition of iodide does not affect the spectrum, probably because of the low affinity of iodide toward zinc. Upon anion addition, the emission band changes in intensity but does not displace its position (Figure 5 and Supporting Information, Figure S6). When 0 to 1 equiv of fluoride or chloride are added, the emission band slightly decreases in intensity. However, it then starts to increase when more than 1 equiv of anion is added, reaching its maximum in the case of chloride at 2 equiv, whereas for the fluoride addition, it also increases after 2 equiv. In contrast, the addition of bromide and iodide quenches the fluorescence. Accordingly, there is a sort of selectivity in the fluorescence response between chloride or fluoride ions and bromide or iodide anions. An interpretation of the behavior of fluoride and chloride can be made in terms of the interaction between the metal ion and the donor atom of the ligands that is perturbed by the coordination of the halide anion. In the range of 0 to 1 equiv, the anion probably bridges the two zinc ions and decreases the bond order with all of the nitrogen donor atoms. This results in a negative balance of the emission intensity because the increase of fluorescence resulting from (NBD)N decoordination was counterbalanced by the PET effect due to the partial decoordination of the six aliphatic amine functions. This resulted in an overall slight decrease of the fluorescence emission. The addition of further halide anions causes a rearrangement of the complex, and each anion binds one zinc atom in a nonbridged way (Figure 6). In this case, the metal−halide interaction is stronger and causes the complete decoordination of the (NBD)N nitrogen atoms, resulting in an increase in emission intensity. This can be confirmed by restoring the absorption CT band at about 490 nm, which is typical of free $H_{-1}L^-$.

dx.doi.org/10.1021/ic5001649 | Inorg. Chem. 2014, 53, 4560−4569

[$Cu_2H_{-1}L$]$^{3+}$. The addition of halide anions to a solution of $[Cu_2H_{-1}L]^{3+}$ does not cause significant variations in the absorption spectrum; only the addition of fluoride results in a modest red shift of 353 cm^{-1} with 5 equiv of anions. The emission band does not change its position but decreases in intensity after the addition of all of the four halide anions, with fluoride being the most effective as a fluorescence quencher. The fact that the emission intensity is affected by the anions means that the complex is able to bind them, but the interaction does not cause significant variations in optical properties, making these complexes less interesting for sensing purposes.

[$Cd_2H_{-1}L$]$^{3+}$. The addition of halide anions to a solution of $[Cd_2H_{-1}L]^{3+}$ causes a radical change in the absorption spectrum; the band at 403 nm disappears, whereas that at 457 nm increases in intensity (Figure 4 and Supporting Information, Figures S7 and S8). This suggests that when the metal ion coordinates the external species a decoordination of the (NBD)N donor atom occurs. The emission band at about 540 nm increases in intensity and reaches its maximum at 2 equiv of halide. It then decreases because of a dynamic quenching effect (Figure 5 and Supporting Information, Figures S9 and S10). All of the four halogens give rise to similar changes both in the absorption and emission spectra, meaning that, in this case, all of them interact with the complex in a similar way. The emission intensity at 2 equiv of anion increased by only 50% for all of the halides, suggesting that for the 2Cd/L system a sort of balance between PET and CT persists during the titration. Upon examining the spectra, after the addition of the anions, the absorption at 457 nm reaches its maximum intensity at 2 equiv of added anions, whereas upon the addition of the first equivalent of the anion, 80% of the maximum was reached. This means that in the dinuclear Cd(II) complex, the first added halide influences the (NBD)N−M interaction more than in the Zn(II) complex. This can be a consequence of the stronger interaction with this nitrogen atom in the Cd(II) complex than in the Zn(II) complex. It may also be due to the fact that the first anion does not bridge the two Cd(II) ions.

Addition Constants. The addition constants of $[Zn_2H_{-1}L]^{3+}$ and $[Cd_2H_{-1}L]^{3+}$ with fluoride, chloride, and bromide, which were calculated by UV−vis and fluorescence titrations, are reported in Table 2. For the $[Zn_2H_{-1}L]^{3+}$ species, there is modest selectivity of about 1 logarithm unit for the addition of the first chloride anion over fluoride and bromide. In the case of the chloride and fluoride additions to the Zn(II) complex, it was also possible to determine the constants through the emission spectra, and their values confirm those calculated by UV−vis spectrophotometry. The $[Cd_2H_{-1}L]^{3+}$ species is more selective for fluoride than for the other halides, as the addition constant of F^- is 2 logarithm units higher than those of chloride and bromide.

Table 2. Addition Constants (Log *K*) of Fluoride, Chloride, and Bromide to $[M_2H_{-1}L]^{3+}$ Complexes in an Acetonitrile/Water 95:5 (v/v) Solution at 298 K

reaction	Log *K*		
	X = F	X = Cl	X = Br
$[Zn_2H_{-1}L]^{3+} + X^- = [Zn_2H_{-1}LX]^{2+}$	5.3(2)[a]	6.7(2)[a]	5.9(3)[a]
	5.3(3)[b]	6.8(3)[b]	
$[Zn_2H_{-1}LX]^{2+} + X^- = [Zn_2H_{-1}LX_2]^{+}$	4.7(2)[a]	5.1(3)[a]	4.9(2)[a]
	4.8(3)[b]	5.7(3)[b]	
$[Cd_2H_{-1}L]^{3+} + X^- = [Cd_2H_{-1}LX]^{2+}$	8.4(2)[a]	6.5(4)[a]	6.3(2)[a]
$[Cd_2H_{-1}LX]^{2+} + X^- = [Cd_2H_{-1}LX_2]^{+}$	6.7(3)[a]	5.2(4)[a]	5.1(3)[a]

[a]Determined from UV−vis titrations. [b]Determined from fluorescence titrations.

Subcellular Localization Studies. In analogy with **L1**, which is able to switch on emission in a cellular context,[13,14] preliminary experiments were carried out using living HeLa cells to evaluate if **L** can be internalized inside cells and may thus have the potential to be used in biological environments as a fluorogenic marker. As reported in Figure 7, $NaH_{-1}L$ is able to bypass the cell membrane and is preferentially accumulated in the cytoplasm. In fact, the nuclei (marked with N in Figure 7b at higher magnification) are excluded from the distribution of the molecule (green). The insertion of the phenol moiety to separate two **L** subunits has maintained the properties exhibited by **L1** to pass through the cell membrane, with the consequence being the switching on of the fluorescence inside the cells.

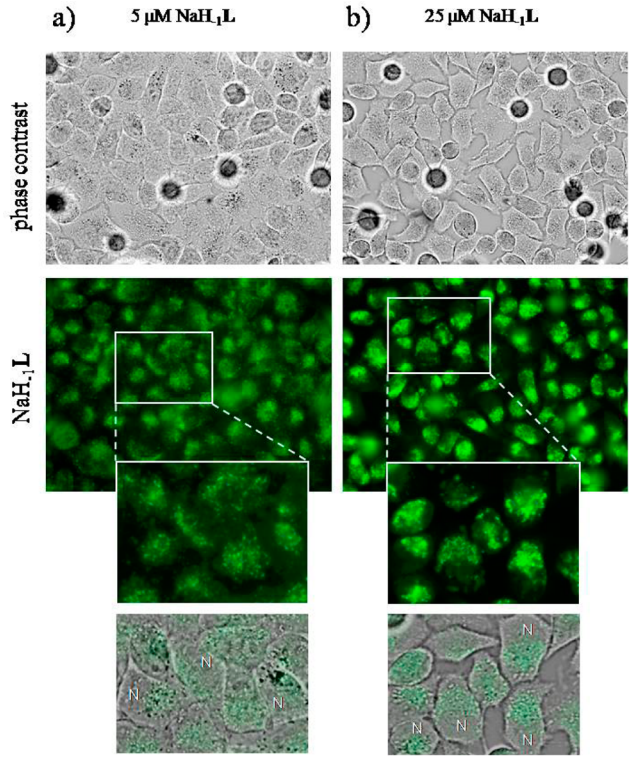

Figure 7. Cellular internalization of $NaH_{-1}L$ by fluorescence microscopy. Living HeLa cells were incubated with $NaH_{-1}L$ at the indicated concentrations for 1 h at 37 °C. Cellular morphology was monitored by phase-contrast observations, and both cellular internalization and the accumulation of $NaH_{-1}L$ were monitored by following the fluorescent signal (green). N, nuclei.

CONCLUDING REMARKS

Ligand **L**, containing two NBD fluorescent units, is able to signal both metal ions and halide anions. It can also pass through the cell membrane, becoming fluorescent inside cells. The $H_{-1}L^-$ species is able to form dinuclear metal complexes in which the oxygen atom of the phenolate moiety bridges the two metal ions, allowing them to stay close to each other and close to the aliphatic amine functions of each macrocyclic subunit. These dinuclear species can behave as metallo-receptors for

dx.doi.org/10.1021/ic5001649 | Inorg. Chem. 2014, 53, 4560−4569

anions; the dinuclear Cu(II), Zn(II), and Cd(II) complexes are able to add one or two halide anions, giving rise to stable adducts, and are able to sense these anions by UV−vis absorption and the fluorescence outcomes.

The photochemical response of the dinuclear complexes to the presence of halide anions depends on the metal ions being coordinated (Figure 8): the Cu(II) complex was quenched by

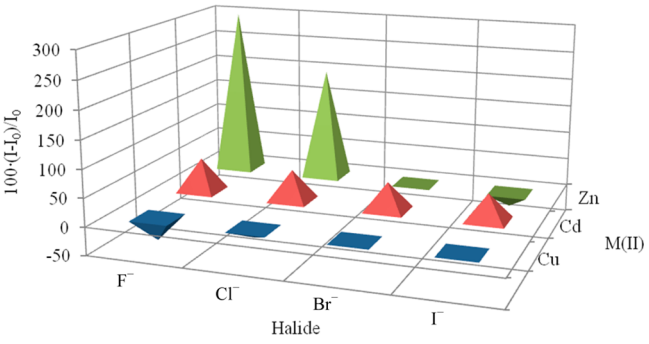

Figure 8. Variation of the emission intensity (%) at 543 nm for the $[M_2H_{-1}L]^{3+}$ complexes (M = Cu, Zn, and Cd) after the addition of 2 equiv of halide anions as tetrabutylammonium salt (acetonitrile/water 95:5 (v/v) solution).

all of the halides; in contrast, the Cd(II) system undergoes an increment of the emission intensity of 1.5 times, notwithstanding the addition of the halogen anion. The most intriguing behavior was shown by the $[Zn_2H_{-1}L]^{3+}$ complex, which showed enhanced fluorescence emission by 300% with the fluoride anion and 200% with the chloride anion but not at all with bromide and iodide. Accordingly, this system reveals a photochemical selectivity toward F^- and Cl^- with respect to the other halides, although the stability of the corresponding adducts is very similar. Nevertheless, as observed in Figure 5, the increase in the emission is rather modest, approximately 3 times, not enough yet to use these systems as practical devices. The assembling of two macrocyclic NBD subunits spaced by the phenol preserved the original properties of the subunits to pass through the cell membrane, switching on the fluorescence inside the cells and thus giving **L** appeal as a chemosensor for biological uses.

EXPERIMENTAL SECTION

General Methods. UV absorption spectra were recorded at 298 K on a Varian Cary-100 spectrophotometer equipped with a temperature control unit. Fluorescence emission spectra were recorded at 298 K on a Varian Cary-Eclipse spectrofluorimeter, and the spectra are uncorrected. ^1H and ^{13}C NMR spectra were recorded at 298 K on a Bruker Avance instrument operating at 200.13 and 50.33 MHz, respectively. For the spectra recorded in acetonitrile-d_3, the peak positions are reported with respect to the solvent residual protons and ^{13}C (1.94 and 1.79 ppm, respectively). All reagents and solvents used were of analytical grade.

X-ray Crystallography. Intensity data for compound $[Cd_2(H_{-1}L)Cl_2](ClO_4)\cdot 4H_2O$ (**2**) were collected on an Oxford Diffraction Excalibur diffractometer using a Cu K_α radiation (λ = 1.54184 Å). The data collection was performed with the program CrysAlis CCD;[31] data reduction was carried out with the program CrysAlis RED,[32] and absorption correction was performed with the program ABSPACK in CrysAlis RED.[33]

The structure was solved by using the SIR-97 package[34] and subsequently refined on the F^2 values by the full-matrix least-squares program SHELXL-97.[35]

All non-hydrogen atoms were anisotropically refined except for atoms O(2WA), O(2WB), O(3WA), O(3WB), O(4WA), and O(4WB), which were introduced with an occupancy factor of 0.5 and therefore isotropically refined.

The hydrogen atoms of the ligand were introduced in calculated positions and isotropically refined with $U_{iso}(H)$ 1.2 times $U_{eq}(C)$ (1.5 for methyl H atoms). The hydrogen atoms belonging to the water molecules were not introduced in the refinement.

Geometrical calculations were performed by PARST97,[36] and molecular plots were produced by the Mercury 2.4[37] and ORTEP3[38] programs.

Crystallographic data and refinement parameters are reported in Table 3.

Table 3. Crystallographic Data and Refinement Parameters for Compound 2

	2
formula	$[Cd_2(H_{-1}L)Cl_2](ClO_4)\cdot 4H_2O$
MW	1311.19
T (K)	150
λ (Å)	1.541 84
crystal system, space group	triclinic, $P\bar{1}$
unit cell dimensions (Å, deg)	a = 14.377(1), α = 62.625(6)
	b =15.1740(8), β = 63.908(7)
	c =15.839(1), γ = 65.876(6)
volume (Å^3)	2661.7(3)
Z, D_c (mg/cm^3)	2, 1.636
μ (mm^{-1})	8.441
F(000)	1336
crystal size (mm)	0.45 × 0.25 × 0.1
2θ range (deg)	8.06−145.26
reflns collected/unique (R_{int})	30 229/10 174(0.0539) ($I > 2\sigma(I)$ = 7310)
data/parameters	10 174/664
final R indices [$I > 2\sigma(I)$]	R1 = 0.0493, wR2 = 0.1197
R indices (all data)	R1 = 0.0821, wR2 = 0.1442
GOF	1.054

Synthesis. Ligand **L1**[16] and 2,6-bis(bromomethyl)phenol (**1**) were synthesized as previously reported.[22]

Sodium 2,6-Bis{[7-(7-nitrobenzo[1,2,5]oxadiazole-4-yl)-3,10-dimethyl-1,4,7,10-tetraazacyclododeca-1-yl]methyl}phenolate ($NaH_{-1}L$). A solution of 40 mL of DMF containing 2,6-bis(bromomethyl)phenol (**1**) (0.40 g, 1.43 mmol) was added dropwise to a suspension of ligand **L1**·4HCl (1.46 g, 2.86 mmol) and K_2CO_3 (4.00 g, 29 mmol) in 40 mL of DMF at 90 °C under nitrogen. The reaction mixture was stirred for a further 6 h at 90 °C. Subsequently, the solution was poured into cold water (500 mL), obtaining a red solid. The product was filtered, washed with water, dried under vacuum, and redissolved in chloroform. The organic solution was filtered and evaporated, obtaining 1.7 g of a red solid (**L**). This solid was dissolved in 15 mL of water and 15 mL of a 37% aqueous HCl mixture. The red solution was filtered, and 200 mL of absolute ethanol was added to precipitate the final product as its hydrochloride salt (**L**·8HCl) as a dark red solid (1.19 g of **L**·8HCl, 73%; Anal. Calcd for **L**·8HCl ($C_{40}H_{64}Cl_8N_{14}O_7$): C, 42.27; H, 5.68; N, 17.25. Found: C, 42.4; H, 5.8; N, 17.1). To obtain the anionic form of the complex, **L**·8HCl was dissolved in 20 mL of water and treated with solid sodium carbonate up to pH 11. The resulting red suspension was extracted with dichloromethane. The evaporation of the solvent afforded pure $NaH_{-1}L$ suitable for photochemical and NMR studies (770 mg of $NaH_{-1}L$, 85% with respect to **L**·8HCl). ^1H NMR ($CDCl_3$, 25 °C): δ 8.35 (2H, d, J = 9.1 Hz, NBD), 7.11 (2H, d, J = 7.5 Hz, Ar), 6,65 (1H, t, J = 7,5 Hz, Ar), 6.13 (2H, d, J = 9.1 Hz, NBD), 4.23 (8H, br, NBD-N−CH_2), 3.60 (4H, s, Ar−CH_2), 2.94 (8H, br, macrocycle), 2.61 (8H, br, macrocycle), 2.55 (8H, br, macrocycle), 2.24 (12H, s, N−CH_3).

dx.doi.org/10.1021/ic5001649 | Inorg. Chem. 2014, 53, 4560−4569

^{13}C NMR ($CDCl_3$, 25): δ 155.7, 145.4, 144.9, 144.5, 135.4, 129.7, 124.4, 121.4, 118.1, 101.3, 55.9, 54.2, 54.1, 51.6, 43.0.

$[Cd_2(H_{-1}L)Cl_2](ClO_4)\cdot 4H_2O$ (2). A sample of $Cd(ClO_4)_2\cdot 6H_2O$ (25 mg, 0.06 mmol) in acetonitrile (5 mL) was added to a solution containing **L**·8HCl (35 mg, 0.03 mmol in 10 mL of water). The pH of the resulting solution was adjusted to 7 with 0.1 M NaOH and saturated with solid $NaClO_4$. After a few minutes, **2** precipitated as a microcrystalline red solid (49 mg, 77%). Anal. Calcd for $C_{40}H_{63}Cl_3N_{14}O_{15}$: C 36.64; H 4.84; N 14.96; Found: C 36.9; H 5.0; N 14.5. Crystals suitable for X-ray analysis were obtained by slow evaporation of an acetonitrile solution containing **2**.

UV–Vis Titrations. At least three sets of spectrophotometric titration curves for each anion/metal complex system were performed. All sets of curves were treated either as single sets or as separate entities for each system; no significant variations were found in the values of the determined constants. The Hyperquad computer program was used to process the spectrophotometric data.[39] For the titration of metal complexes with halide anions, in a typical experiment, aliquots of 0.100 mL of 1.25×10^{-3} mol·dm^{-3} acetonitrile solution of the halide as tetrabuthylammonium salt were added to 25 mL of a 5×10^{-5} mol·dm^{-3} acetonitrile/water 95:5 (v/v) solution of the preformed metal complex, obtained by dilution of the stock solution. The titration vase was then kept for 5 min at 298 K before starting the acquisition of the spectrum.

NMR Titrations. NMR titrations were carried out in acetonitrile-d_3 solution. For the titration of the ligand with metal ions, in a typical experiment, a 5×10^{-2} mol·dm^{-3} acetonitrile-d_3 solution of the metal ion as its perchlorate salt was added 0.1 equiv at a time to a 1×10^{-2} mol·dm^{-3} acetonitrile-d_3 solution of the ligand directly in the NMR tube; the tube was then kept for 5 min at 298 K before starting the acquisition of the spectrum. For the titration of metal complexes with halide anions, in a typical experiment, a 5×10^{-2} mol·dm^{-3} acetonitrile-d_3 solution of the halide as a tetrabuthylammonium salt was added 0.1 equiv at a time to a 1×10^{-2} mol·dm^{-3} acetonitrile-d_3 solution of the preformed metal complex directly in the NMR tube; the tube was then kept for 5 min at 298 K before starting the acquisition of the spectrum.

Cell Culture, Treatments, and Fluorescence Microscopy. Human cervical carcinoma HeLa cells were obtained from the American Type Culture Collection (ATTC). Cells were grown in DMEM (Lonza) supplemented with fetal bovine serum (10%), penicillin/streptomycin (1%), and glutamine (1%) and were cultured in a humidified atmosphere at 37 °C, as previously described.[40]

Cells were plated in 8-well Permanox slides (Nalge–Nunc International) 16 h before the start of the experiments to reach about 60–70% confluence.

NaH_{-1}**L** was dissolved at a final concentration of 10 mM in dimethyl sulfoxide and subsequently diluted in cell culture medium just before use. Cells were treated for 1 h at the indicated concentrations and then washed twice with phosphate-buffered saline (1× PBS). Acquisition of fluorescence signal was carried out in cell culture medium, without cell fixation, using an Olympus BX51 microscope equipped with an Olympus F-View digital camera and AnalySIS software (Soft Imaging System, GmbH), as previously described.[41]

■ ASSOCIATED CONTENT

Ⓢ Supporting Information

^{1}H NMR spectrum of free NaH_{-1}**L** species, UV–vis and fluorescence titration spectra, and crystallographic data in CIF format for compound **2**. This material is available free of charge via the Internet at http://pubs.acs.org.

■ AUTHOR INFORMATION

Corresponding Author

*E-mail: vieri.fusi@uniurb.it. Tel/Fax: +39-0722-350032.

Notes

The authors declare no competing financial interest.

■ ACKNOWLEDGMENTS

We thank the Italian Ministero dell'Istruzione dell'Università e della Ricerca (MIUR), PRIN2009 for financial support as well as the Centro di Crystallografia Strutturale (CRIST, University of Firenze), where X-ray data was collected.

■ REFERENCES

(1) Davis, F.; Collyer, S. D.; Higson, S. P. J. *Top. Curr. Chem.* **2005**, *255*, 97–124.
(2) Lavis, L. D.; Raines, R. T. *ACS Chem. Biol.* **2008**, *3*, 142–155.
(3) Jagt, R. B. C.; Kheibari, M. S.; Nitz, M. *Dyes Pigm.* **2009**, *81*, 161–165.
(4) Zhang, Y. M.; Lin, Q.; Wei, T. B.; Wang, D. D.; Yao, H.; Wang, Y. L. *Sens. Actuators, B* **2009**, *137*, 447–455.
(5) Graefe, A.; Stanca, S. E.; Nietzsche, S.; Kubicova, L.; Beckert, R.; Biskup, C.; Mohr, G. J. *Anal. Chem.* **2008**, *80*, 6526–6531.
(6) Ruedas-Rama, M. J.; Hall, E. A. H. *Analyst* **2008**, *133*, 1556–1566.
(7) Kim, U. I.; Suk, J. M.; Naidu, V. R.; Jeong, K. S. *Chem.—Eur. J.* **2008**, *14*, 11406–11414.
(8) Gale, P. A. *Chem. Commun.* **2008**, 4525–4540.
(9) Schazmann, B.; Alhashimy, N.; Diamond, D. *J. Am. Chem. Soc.* **2006**, *128*, 8607–8614.
(10) Geddes, C. D. *Meas. Sci. Technol.* **2001**, *12*, R53–R88.
(11) Gassensmith, J. J.; Matthys, S.; Lee, J. J.; Wojcik, A.; Kamat, P. V.; Smith, B. D. *Chem.—Eur. J.* **2010**, *16*, 2916–2921.
(12) Riis-Johannessen, T.; Schenk, K.; Severin, K. *Inorg. Chem.* **2010**, *49*, 9546–9556.
(13) Amatori, S.; Ambrosi, G.; Fanelli, M.; Formica, M.; Fusi, V.; Giorgi, L.; Macedi, E.; Micheloni, M.; Paoli, P.; Pontellini, R.; Rossi, P.; Varrese, M. A. *Chem.—Eur. J.* **2012**, *18*, 4274–4284.
(14) Ambrosi, G.; Ciattini, S.; Formica, M.; Fusi, V.; Giorgi, L.; Macedi, E.; Micheloni, M.; Paoli, P.; Rossi, P.; Zappia, G. *Chem. Commun.* **2009**, *45*, 7039–7041.
(15) Ceccanti, N.; Formica, M.; Fusi, V.; Giorgi, L.; Micheloni, M.; Pardini, R.; Pontellini, R.; Tinè, M. R. *Inorg. Chim. Acta* **2001**, *321*, 153–161.
(16) Dapporto, P.; Formica, M.; Fusi, V.; Giorgi, L.; Micheloni, M.; Paoli, P.; Pontellini, R.; Rossi, P. *Inorg. Chem.* **2001**, *40*, 6186–6192.
(17) Formica, M.; Fusi, V.; Giorgi, L.; Micheloni, M.; Palma, P.; Pontellini, R. *Eur. J. Org. Chem.* **2002**, 402–404.
(18) Formica, M.; Giorgi, L.; Fusi, V.; Micheloni, M.; Pontellini, R. *Polyhedron* **2002**, *21*, 1351–1356.
(19) Ambrosi, G.; Dapporto, P.; Formica, M.; Fusi, V.; Giorgi, L.; Guerri, A.; Micheloni, M.; Paoli, P.; Rossi, P. *J. Supramol. Chem.* **2002**, *2*, 301–303.
(20) Berti, E.; Caneschi, A.; Daiguebonne, C.; Dapporto, P.; Formica, M.; Fusi, V.; Giorgi, L.; Guerri, A.; Micheloni, M.; Paoli, P.; Pontellini, R.; Rossi, P. *Inorg. Chem.* **2003**, *42*, 348–357.
(21) Ambrosi, G.; Formica, M.; Fusi, V.; Giorgi, L.; Guerri, A.; Macedi, E.; Micheloni, M.; Paoli, P.; Pontellini, R.; Rossi, P. *Inorg. Chem.* **2009**, *48*, 5901–5912.
(22) Salo, T. M.; Helaja, J.; Koskinen, A. M. P. *Tetrahedron Lett.* **2006**, *17*, 2977–2980.
(23) Das, S.; Hung, C. H.; Goswami, S. *Inorg. Chem.* **2003**, *42*, 8592.
(24) Karunakaran, C.; Justin Thomas, K. R.; Shunmugasundaram, A.; Murugesan, R. *J. Chem. Crystallogr.* **1999**, *29*, 413–420.
(25) Allen, F. H. *Acta Crystallogr.* **2002**, *B58*, 380–388.
(26) (a) Heyrovska, R. *Mol. Phys.* **2005**, *103*, 877–882. (b) Bondi, A. *J. Phys. Chem.* **1964**, *68*, 441–451. (c) Huheey, J. E.; Keiter, E. A.; Keiter, R. L. *Inorganic Chemistry: Principles of Structure and Reactivity*, 4th ed.; Harper Collins: New York, 1993; pp 114 and 292. (d) *CRC Handbook of Chemistry and Physics*, 78th ed.; Lide, D. R., Ed.; CRC Press: Boca Raton, FL, 1997; pp 12–14.
(27) (a) Yang, F. A.; Chen, J. H.; Hsieh, H. Y.; Elango, S.; Hwang, L. P. *Inorg. Chem.* **2003**, *42*, 4603–4609. (b) Fondo, M.; Sousa, A.; Bermejo, M. R.; Garcia-Deibe, A.; Sousa-Pedrares, A.; Hoyos, O. L.;

Helliwell, M. *Eur. J. Inorg. Chem.* **2002**, *3*, 703−710. (c) Du, M.; Chen, S. T.; Bu, X. H. *Cryst. Growth Des.* **2002**, *2*, 665−673.
(28) Bernal, I. *Stereochemistry of organometallic and inorganic compounds*; Elsevier: Amsterdam, The Netherlands, 1987; Vol. 2.
(29) The Gaussian 03 (revision C.02) package was used. All of the studied species were fully optimized using density functional theory (DFT) method by means of Becke's three-parameter hybrid method with the LYP correlation functional. The effective core potential of Hay and Wadt was used for the palladium atom. The 6-31G* basis set was used for the remaining atomic species. Starting geometries for the modeled species were based on the solid-state structures of $[Cd_2H_{-1}LCl_2]^+$ and $[CuL1Cl]^+$. Both of the optimized species retain the L_{in} and L_{out} disposition of the NBD moieties with respect to the metal ions and the trends in the Cd-donor atoms bond distances of the parent experimental compounds.
(30) (a) Uchiyama, S.; Santa, T.; Fukushima, T.; Homma, H.; Imai, K. *J. Chem. Soc., Perkin Trans. 2* **1998**, 2165−2173. (b) Uchiyama, S.; Santa, T.; Imai, K. *J. Chem. Soc., Perkin Trans. 2* **1999**, 569−576.
(31) *CrysAlis CCD*, version 1.171.36.28; Oxford Diffraction Ltd.: Abingdon, England, 2013.
(32) *CrysAlis RED*, version 1.171.36.28; Oxford Diffraction Ltd.: Abingdon, England, 2013.
(33) *ABSPACK in CrysAlis RED*, version 1.171.36.28; Oxford Diffraction Ltd.: Abingdon, England, 2013.
(34) Altomare, A.; Cascarano, G. L.; Giacovazzo, C.; Guagliardi, A.; Burla, M. C.; Polidori, G.; Camalli, M. *J. Appl. Crystallogr.* **1999**, *32*, 115−119.
(35) Sheldrick, G. M. *SHELX 97*; University of Göttingen: Göttingen, Germany, 1997.
(36) Nardelli, M. *J. Appl. Crystallogr.* **1995**, *28*, 659−662.
(37) Macrae, C. F.; Bruno, I. J.; Chisholm, J. A.; Edgington, P. R.; McCabe, P.; Pidcock, E.; Rodriguez-Monge, L.; Taylor, R.; van de Streek, J.; Wood, P. A. *J. Appl. Crystallogr.* **2008**, *41*, 466−470.
(38) Farrugia, L. J. *J. Appl. Crystallogr.* **1997**, *30*, 565.
(39) Gans, P.; Sabatini, A.; Vacca, A. *Talanta* **1996**, *43*, 1739−1753.
(40) Amatori, S.; Papalini, F.; Lazzarini, R.; Donati, B.; Bagaloni, I.; Rippo, M. R.; Procopio, A.; Pelicci, P. G.; Catalano, A.; Fanelli, M. *Lung Cancer* **2009**, *66*, 184−190.
(41) Amatori, S.; Bagaloni, I.; Viti, D.; Fanelli, M. *Lung Cancer* **2011**, *71*, 113−115.

dx.doi.org/10.1021/ic5001649 | *Inorg. Chem.* 2014, 53, 4560−4569